2025 IMEKO TC-6 International Conference on
Metrology and Digital Transformation - **M4DConf 2025**
Benevento, Italy, September 3-5, 2025

A Modular Windows-Based Intelligent API for Traceable Drone Positioning Using UWB-OptiTrack Fusion and AI-Based Residual Learning

Ihtisham Ul Haq[1], Luigi D'Alfonso[1], Giuseppe Fedele[1], Francesco Lamonaca[1, 2]

[1]*Department of Computer Science, Modelling, Electronics and Systems (DIMES), University of Calabria, 87036 Rende, CS, Italy*
[2]*National Research Council Institute of Nanotechnology (CNR-NANOTEC), Rende, 87036, Italy*

***Abstract* – Accurate and traceable drone positioning is crucial for autonomous aerial navigation, especially in GNSS-denied environments. Traditional approaches using Ultra-Wideband (UWB) sensors or Kalman Filters (KF) struggle with multipath interference, non-line-of-sight, and environmental uncertainties, and are often limited to Linux-based Application Programming Interfaces (APIs). This work presents an innovative framework based on: a novel modular Windows-based API for real-time drone positioning, the integration of Kalman filter for optimal multi-sensor data fusion and trajectory smoothing, AI-driven residual learning to correct systematic estimation errors, and metrology-compliant uncertainty modeling. The system enables real-time swarm deployment and pose-aware feedback using an auxiliary vision based positiong system (OptiTrack) and UWB data. A feed-forward neural network compensates for residual errors in Kalman-filtered trajectories, while Monte Carlo simulations establish traceable 95% confidence intervals. Experimental tests show that the proposed framework reduces RMSE by over 40% across axes, with strong regression accuracy greater than 94%.**

I. INTRODUCTION

Accurate drone positioning is essential for autonomous navigation, industrial inspection, swarm coordination, and environmental monitoring. While GPS-based methods are widely used, their effectiveness declines in cluttered or indoor environments. Ultra-Wideband (UWB) technology provides high temporal resolution and robustness to multipath interference, making it suitable for such settings [1, 2, 3]. However, UWB systems may still experience performance degradation in non-line-of-sight (NLoS) conditions and are sensitive to calibration biases, leading to trajectory distortions and time-varying errors [4, 19, 6].

Probabilistic filtering approaches such as the Kalman Filter (KF) and its nonlinear extensions (EKF, UKF) are often applied to mitigate these issues through multi-sensor data fusion [7, 8]. Yet, their accuracy can be limited by Gaussian noise and linearity assumptions that are not always met in real-world scenarios [9, 8]. Recent work leverages Artificial Neural Networks (ANNs) to model and correct complex error patterns in UWB-based positioning, using metrological ground truth from systems such as OptiTrack [10, 19, 11]. Embedding metrological principles, bias quantification, and uncertainty modeling has further advanced measurement accuracy and reliability [8, 19, 3].

For drone swarms, real-time synchronization and scalable multi-agent fusion are crucial. Modular APIs support decentralized UWB-OptiTrack integration and enable robust swarm operations [11, 12]. Sensor fusion strategiesâcombining UWB, IMU, and barometric data with AI models such as multilayer perceptrons offer resilience against sensor drift and dynamic conditions [9, 13]. However, a fully integrated, standards-oriented framework for filtering, AI correction, and metrological uncertainty remains lacking.

This work introduces a unified, modular positioning framework that combines Kalman filtering, ANN-based residual correction, and rigorous metrological uncertainty modeling for traceable, real-time positioning of both individual drones and swarms. UWB and OptiTrack data are fused via ANNs and Monte Carlo-based assessment. The remainder of this paper is structured as follows: Section ii. presents the methodology, Section iii. reports experimental results, and Section iv. discusses conclusions and future work.

II. DRONE TRAJECTORY REFINEMENT AND API INTEGRATION

It is proposed a robust framework that integrates OptiTrack (OT) motion capture [15] and Ultra Wideband (UWB) modules for accurate drone trajectory estimation and benchmarking via a modular, decentralized API. The pipeline consists of intelligent data acquisition, Kalman-filtered state estimation, uncertainty quantification, AI-based residual learning, and ensemble fusion. Fig. 1 out-

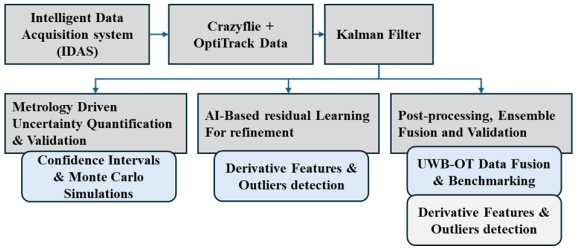

Fig. 1. Block scheme of the proposed framework for drone trajectory refinement.

lines the complete process.

The Intelligent Data Acquisition System (iDAS) module is used to synchronize and record positional data from Crazyflie drones [16] with both UWB and OptiTrack sensors. Real-time data streaming is enabled through a MATLAB-based API, interfacing with the NatNet SDK [17] and UWB radio modules [18].

A. Kalman Filter for Position Estimation

To fuse noisy measurements from multiple sources, a linear Kalman Filter (KF) is used with the standard discrete-time state-space model:

$$\mathbf{x}_k = \mathbf{A}\mathbf{x}_{k-1} + \mathbf{B}\mathbf{u}_{k-1} + \mathbf{w}_{k-1}, \tag{1}$$

$$\mathbf{z}_k = \mathbf{H}\mathbf{x}_k + \mathbf{v}_k, \tag{2}$$

where $\mathbf{x}_k$ is the 6-DOF state vector defined as $\mathbf{x}_k = [x_k,\, y_k,\, z_k,\, \dot{x}_k,\, \dot{y}_k,\, \dot{z}_k]^\top \in R^6$, representing the three-dimensional position and velocity components (positions and speeds in R^3). The control input $\mathbf{u}_{k-1} = [u_x,\, u_y,\, u_z]^\top \in R^3$ typically denotes commanded accelerations or velocity increments. The state transition matrix $\mathbf{A} \in R^{6\times6}$ and control input matrix $\mathbf{B} \in R^{6\times3}$ are structured for a constant-velocity motion model, while the measurement matrix $\mathbf{H} \in R^{3\times6}$ extracts the position components from the state vector. The process noise $\mathbf{w}_{k-1} \sim \mathcal{N}(0,\, \mathbf{Q})$ and measurement noise $\mathbf{v}_k \sim \mathcal{N}(0,\, \mathbf{R})$ are assumed to be zero-mean, mutually uncorrelated Gaussian random vectors, with covariances $\mathbf{Q}$ and $\mathbf{R}$, respectively. The matrix sizes are: $\mathbf{x}_k \in R^6$, $\mathbf{u}_{k-1} \in R^3$, $\mathbf{A} \in R^{6\times6}$, $\mathbf{B} \in R^{6\times3}$, $\mathbf{z}_k \in R^3$, and $\mathbf{H} \in R^{3\times6}$.

$$\mathbf{w}_{k-1} \sim \mathcal{N}(0, \mathbf{Q}),\ \mathbf{v}_k \sim \mathcal{N}(0, \mathbf{R}),\ E\left[\mathbf{w}_{k-1}\mathbf{v}_j^\top\right] = 0\ \forall k, j. \tag{3}$$

B. AI-Based Refinement, Anomaly Detection, and Fusion Benchmarking

Residual errors from Kalman-filtered trajectories are adaptively corrected using a feed-forward neural network that models the residual as

$$\mathbf{e}_k = \hat{\mathbf{x}}_k^{KF} - \mathbf{x}_k^{GT}, \quad \hat{\mathbf{e}}_k = \mathcal{F}_\theta(\mathbf{z}_k), \tag{4}$$

with the refined estimate given by

$$\mathbf{x}_k^{ref} = \hat{\mathbf{x}}_k^{KF} - \hat{\mathbf{e}}_k. \tag{5}$$

To further enhance robustness, time-aware profiling is conducted by computing velocity and acceleration,

$$v_k = \frac{x_k - x_{k-1}}{\Delta t}, \quad a_k = \frac{v_k - v_{k-1}}{\Delta t}, \tag{6}$$

and applying z-score-based outlier rejection ($|z| > 3$) to eliminate noisy or delayed measurements. Refined position estimates from UWB and OptiTrack (OT) are then fused via weighted averaging,

$$\mathbf{x}_f = w_{UWB} \cdot \mathbf{x}_{UWB} + w_{OT} \cdot \mathbf{x}_{OT}, \tag{7}$$

followed by an ensemble mean fusion to yield the final trajectory:

$$\mathbf{x}_{final} = \frac{1}{M}\sum_{i=1}^{M} \mathbf{x}_i^{(ref)}. \tag{8}$$

Here, $\mathbf{x}_{final}$ denotes the final fused trajectory estimate, M is the total number of estimation models or fusion sources, and $\mathbf{x}_i^{(ref)}$ represents the i-th refined trajectory estimate contributed by each model or fusion branch. Performance is validated using Root Mean Squared Error (RMSE), Standard Deviation (SD), and 95% confidence coverage, ensuring the methodology provides traceable, adaptive, and high-fidelity trajectory estimation through heterogeneous sensing and metrologically rigorous fusion.

Algorithm 1 Unified Framework for Trajectory Refinement and Swarm Execution

Require: Drone set $\mathcal{D}$, OptiTrack and UWB modules, model parameters

Initialize: Synchronize clocks; activate sensor streams; assign unique IDs for $d \in \mathcal{D}$
Register pose acquisition callbacks and prepare logging
Synchronize: Wait for all drones to reach ready state
while mission is active **do**
  for all drone $d \in \mathcal{D}$ **(in parallel) do**
    Obtain sensor measurements $\mathbf{z}_k^{(d)}$ (UWB, OT)
    State Estimation: Fuse via Kalman filter *(Eqs. 1–2)*
    Uncertainty Quantification: Monte Carlo + CI *(Eqs. 3–4)*
    Outlier Removal: Velocity/acceleration profile, z-score threshold
    Residual Correction: AI-based learning *(Eq. 5)*
    Multi-Sensor Fusion: Weighted average *(Eq. 6)*, ensemble mean *(Eq. 7)*
    Issue control setpoints; log data for validation
  end for
end while
Finalize: Stop logging; disconnect; evaluate RMSE, SD, CI coverage =0

III. RESULTS AND DISCUSSION

The proposed framework was experimentally validated for drone trajectory estimation using UWB and OptiTrack systems, with further refinement via artificial neural networks (ANNs). The following analysis presents quantitative and visual results, including error metrics, uncertainty quantification, and ANN-based correction, to assess positioning fidelity and system robustness.

A. *UWB and OptiTrack-Based Trajectory Evaluation*

Figure 2 illustrates the Crazyflieâs UWB-based trajectory across X, Y, and Z axes, revealing minor noise and Y-axis drift, as well as step changes in altitude. Despite these variances, the overall movement trend is captured well, supporting the operational viability of the UWB-based estimator. Figure 3 presents the OptiTrack-estimated trajectory in X, Y, and Z, exhibiting smooth and continuous position traces with well-defined altitude steps and stable lateral motion. This reflects the systemâs stable tracking and strong temporal consistency throughout the experiment.

B. *Error Characterization Between UWB and OT*

Figure 4 presents the positional error (OT - CF) along all three axes. The X-axis shows moderate error oscillations peaking at ± 0.2 m, while the Y-axis reveals a pronounced negative bias of approximately -0.35 m, suggesting consistent underestimation by the UWB system. The Z-axis error remains within ± 0.05 m, highlighting better alignment during vertical maneuvers.

Figure 5 overlays OT and CF trajectories, clearly contrasting the precise OT path with the slightly lagging UWB estimates. This overlay further substantiates the systematic deviation in the Y-axis and confirms the capacity for correction via residual learning. Figure 6 displays a 3D trajectory overlay, where the CF (dashed red) and OT (solid blue) paths are juxtaposed. Discrepancies are particularly evident in lateral movements, highlighting the need for trajectory correction to reduce spatial offset and maintain consistent spatial alignment.

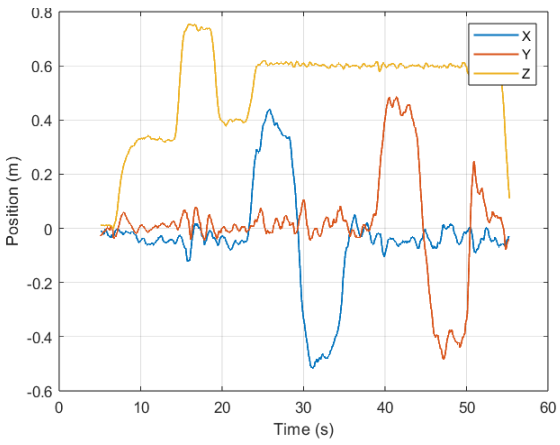

Fig. 2. UWB Based Crazyflie Estimated Trajectories

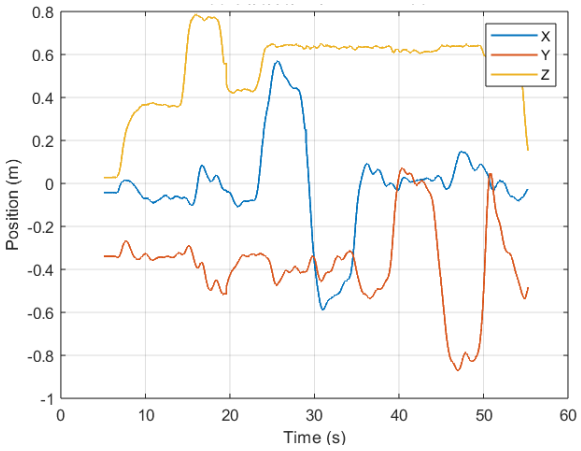

Fig. 3. OptiTrack Estimated Trajectories

C. *Statistical Error Distribution and Uncertainty Estimation*

Figure 7 offers histograms of the positional errors. The X-axis error is centered around 0.025 m, whereas the Y-axis exhibits a negatively skewed distribution peaking at -0.35 m, consistent with prior observations. Z-axis errors remain narrowly centered, indicating relatively accurate height estimation by the UWB module. Figure 8 demonstrates the outcome of a Monte Carlo-based uncertainty quantification, wherein 1000 random trials computed the standard deviation of error vectors. The mean uncertainties are approximately 0.045 m (X), 0.065 m (Y), and 0.012 m (Z). The Y-axis again shows the largest variability, reinforcing its susceptibility to error due to lateral drift or antenna positioning misalignment.

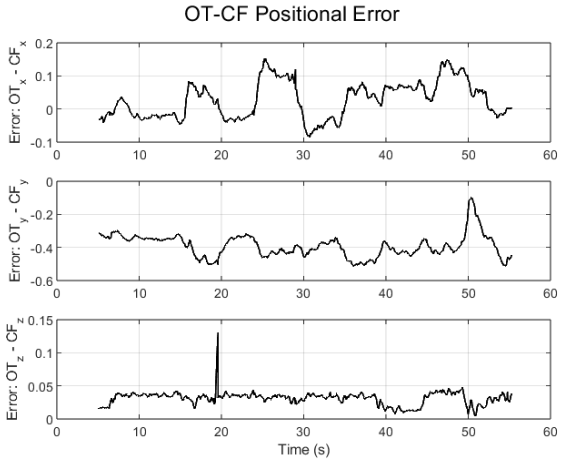

Fig. 4. OT - CF Positional Errors in X, Y, Z Dimensions

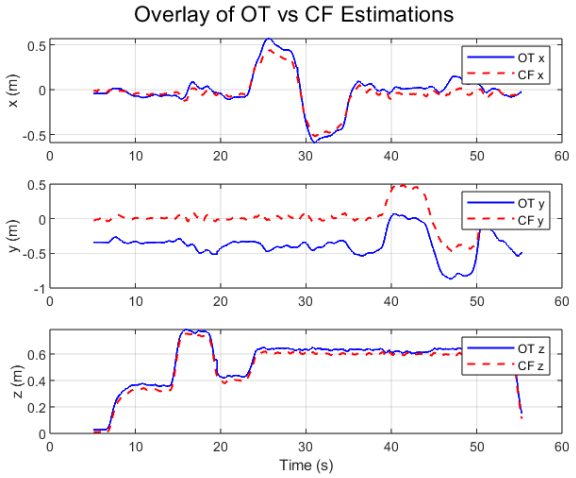

Fig. 5. Overlay of OT vs. CF Trajectory Estimations

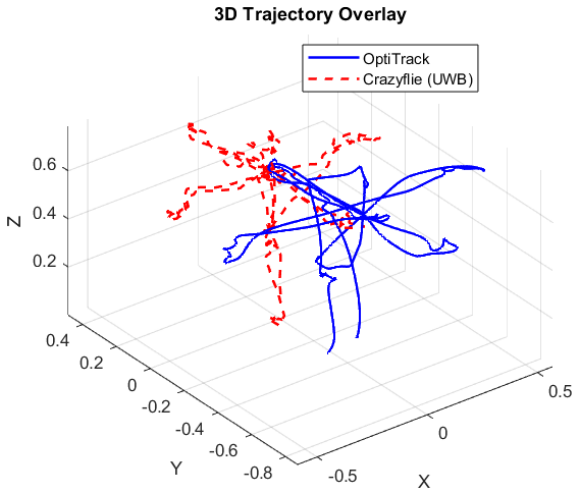

Fig. 6. 3D Trajectory Overlay of UWB and OptiTrack Estimations

D. AI-Based Residual Learning for Estimation Refinement

Figure 9 introduces the AI-enhanced refinement using a shallow ANN, where the green line shows the corrected CF estimates. The ANN-learned residuals successfully align the CF trajectory with the OT ground truth across all axes. The Y-axis correction is especially notable, reducing the systematic bias and enhancing fidelity.

E. ANN Training Performance and Regression Validation

Figure 10 shows the mean squared error (MSE) curves for training, validation, and test sets over 122 epochs, with the minimum validation MSE (0.0053) attained at epoch 116, reflecting strong convergence and negligible overfitting. The log-scale Y-axis highlights a two-order magnitude error reduction, evidencing the effectiveness of the

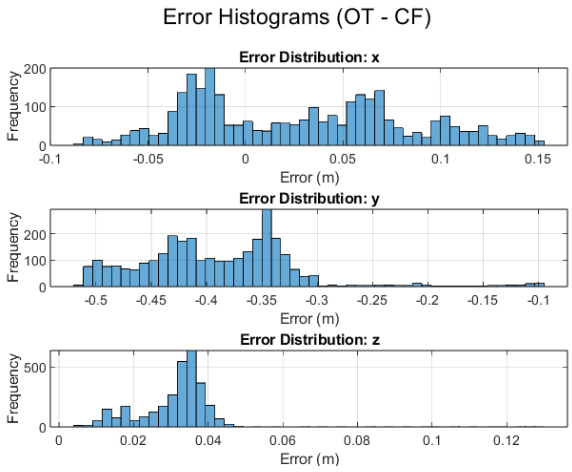

Fig. 7. Error Histogram Distribution Between OT and CF

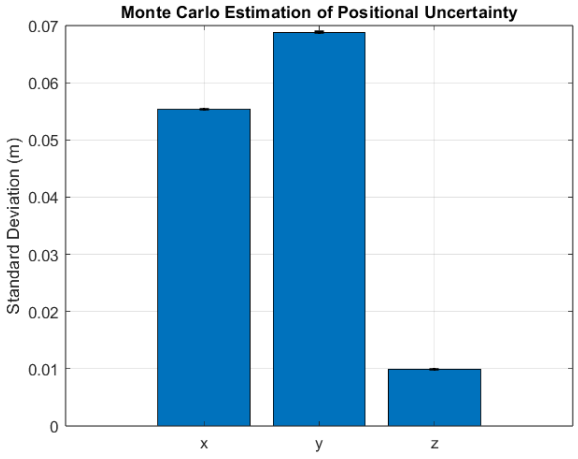

Fig. 8. Monte Carlo-Based Positional Uncertainty Quantification

shallow ANN for residual learning. Following the approach in [19], the network employs three fully connected layers with ReLU activations and a linear output to transform the three-dimensional residual input into a corrected $[x, y, z]$ position. Figure 11 illustrates the internal training dynamics, where the gradient plot confirms stable optimization, and the adaptive μ plot demonstrates efficient convergence via the Levenberg-Marquardt algorithm. The early stopping criterion, triggered after six consecutive validation check failures, effectively prevents overfitting.

Figure 12 plots the distribution of residual errors (Target - Output) for training, validation, and test sets. The concentration of errors around zero suggests the model effectively learned the mapping from UWB positions to correction residuals. No significant bias or skew is observed, indicating balanced learning across all splits. Figure 13 displays correlation plots between predicted residuals and ground truth across training ($R = 0.947$), validation ($R = 0.933$), test ($R = 0.943$), and aggregated

datasets ($R = 0.945$), where R is the Pearson correlation coefficient. The consistently high R-values and close alignment along the diagonal confirm the ANN robust generalization and predictive performance.

The proposed methodology outperforms the one without the refinement across all metrics, including RMSE, MAE and CI coverage (Table 1). The proposed AI-driven framework achieves over 56% reduction in Y-axis RMSE and tighter 95% confidence intervals, underscoring enhanced positional accuracy. These results substantiate the effectiveness of combining metrological validation with AI-based correction for robust, high-precision swarm localization, establishing the MATLAB API as a practical tool for traceable positioning in metrology-driven and multi-agent systems.

Table 1. Comparison of Positional Accuracy Metrics Before and After AI Refinement

Axis	Before Refinement (KF)			After Refinement (KF + AI)		
	RMSE (m)	MAE (m)	CI95 (m)	RMSE (m)	MAE (m)	CI95 (m)
X	0.0462	0.0364	±0.057	0.0241	0.0189	±0.038
Y	0.0678	0.0511	±0.068	0.0295	0.0237	±0.046
Z	0.0254	0.0203	±0.017	0.0106	0.0079	±0.009

F. Comparison with Prior ANN-Based Compensation Methods

Recent advances in neural network-based compensation for UWB and sensor fusion systems have improved positioning accuracy, but key limitations remain in the literature. For example, Chen and Kia [19] achieved a 35% RMSE reduction using a feedforward ANN for UWB-OptiTrack bias correction, yet did not address metrological uncertainty or multi-agent scenarios. Almassri et al. [10] and Bao et al. [9] reported accuracy improvements via ANN and MLP-based approaches; however, their studies lacked formal uncertainty quantification and deployment in traceable, real-world settings. Salimpour et al. [11] proposed autoencoder-based UWB anomaly detection, but did not consider metrological traceability or coordinated swarm control. In contrast, the present work integrates feedforward ANN residual learning with Monte Carlo-driven uncertainty analysis in a modular Windows/MATLAB API, achieving over 56% RMSE reduction on the Y-axis, reporting confidence intervals, and enabling traceable, real-time multi-agent localization. This represents a significant advancement in both technical and operational applicability over previous methods.

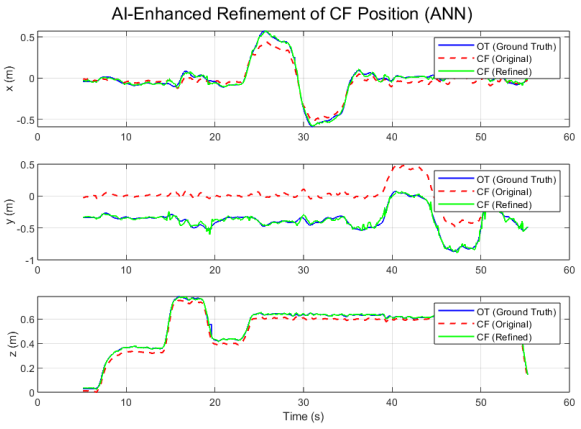

Fig. 9. ANN-Based Residual Learning for Refined Estimation

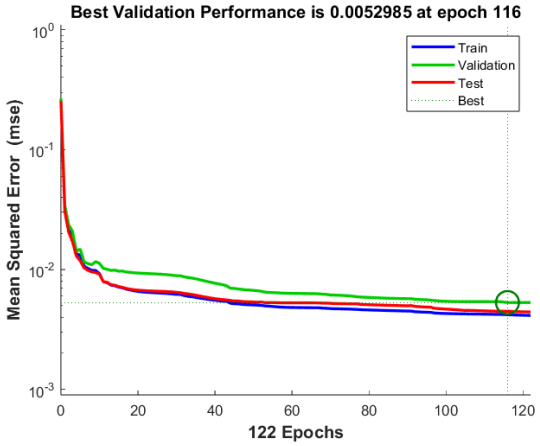

Fig. 10. ANN Training Performance Curve

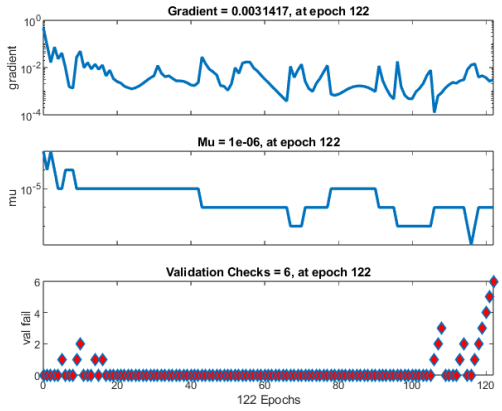

Fig. 11. ANN Training State Metrics (Gradient, Mu, Fail Checks)

IV. CONCLUSION

This work introduced a modular, Windows-based framework for traceable drone positioning, unifying Kalman filtering, AI-driven residual correction, and uncertainty quantification. By leveraging UWB and OptiTrack data

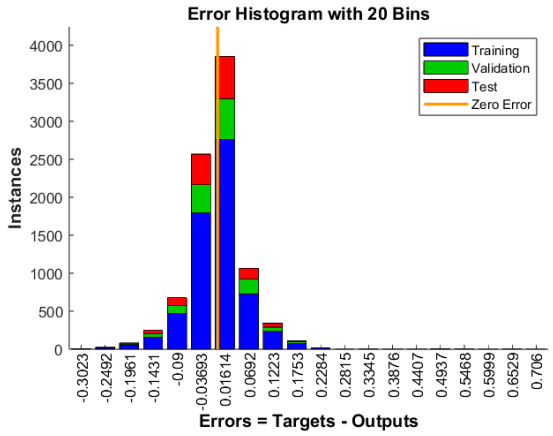

Fig. 12. ANN Residual Error Histogram

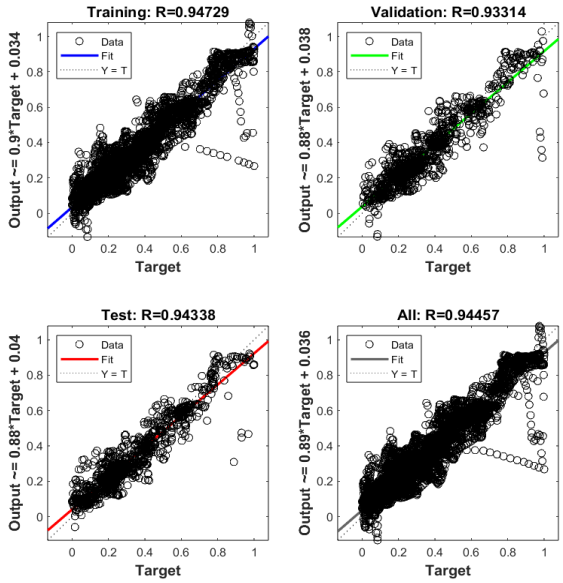

Fig. 13. ANN Regression Analysis Across All Data Splits

within a real-time MATLAB API, the approach enables robust, scalable localization for both individual and swarm drones. Experimental results confirm significant accuracy gainsâover 56% Y-axis RMSE reduction and tighter confidence intervals, demonstrating the effectiveness of integrating AI with metrological approach. The systemâs modular design, comprehensive uncertainty modeling, and realtime swarm execution advance the state-of-the-art for accurate drone positioning in complex environments. Future directions include extending sensor fusion to vision-based and inertial modalities, enhancing adaptive filtering, and further aligning with ISO metrology standards to enable broader certification and deployment in autonomous robotics.

REFERENCES

[1] L. KramariÄ, N. JeluÅ¡iÄ, T. RadiÅ¡iÄ, M. MuÅ¡tra, "A Comprehensive Survey on Short-Distance Localization of UAVs," *Drones*, vol. 9, no. 3, p. 188, Mar. 2025.

[2] W. Shule, C.M. Almansa, J.P. Queralta, Z. Zou, T. Westerlund, "UWB-based localization for multi-UAV systems and collaborative heterogeneous multi-robot systems," *Procedia Comput. Sci.*, vol. 175, pp. 357â364, Jan. 2020.

[3] A. Krummenauer, V.E. Gomes, V.C. Nardelli, "Estimation of Measurement Uncertainty of the Real-Time Location System (RTLS) with Ultra-Wideband (UWB) Technology," *Metrology*, vol. 3, no. 2, pp. 113â130, Mar. 2023.

[4] M.A. Shalaby, C.C. Cossette, J.R. Forbes, J. Le Ny, "Calibration and uncertainty characterization for ultra-wideband two-way-ranging measurements," in *Proc. IEEE Int. Conf. Robot. Autom. (ICRA)*, May 2023, pp. 4128â4134.

[5] C. Chen, S.S. Kia, "OptiTrack-Aided Supervised Learning for Neural Network-Based Ultra-Wideband Ranging Bias Correction," *IEEE Sensors J.*, vol. 24, no. 6, pp. 8484â8492, Feb. 2024.

[6] F. Ma, J. He, X. Zhang, "Robust Kalman filter algorithm based on generalized correntropy for ultra-wideband ranging in industrial environment," *IEEE Access*, vol. 7, pp. 27490â27500, Feb. 2019.

[7] L. MarkoviÄ, M. KovaÄ, R. Milijas, M. Car, S. Bogdan, "Error state extended Kalman filter multi-sensor fusion for unmanned aerial vehicle localization in GPS and magnetometer denied indoor environments," in *Proc. Int. Conf. Unmanned Aircraft Syst. (ICUAS)*, Jun. 2022, pp. 184â190.

[8] J. Jia, K. Guo, W. Li, X. Yu, L. Guo, "Composite filtering for UWB-based localization of quadrotor UAV with skewed measurements and uncertain dynamics," *IEEE Trans. Instrum. Meas.*, vol. 71, pp. 1â3, Feb. 2022.

[9] B. Bao, C. Luo, Y. Hong, Z. Chen, X. Fan, "High-Precision UAV Positioning Method Based on MLP Integrating UWB and IMU," *Tsinghua Sci. Technol.*, vol. 30, no. 3, pp. 1315â1328, Dec. 2024.

[10] A.M. Almassri, N. Shirasawa, A. Purev, K. Uehara, W. Oshiumi, S. Mishima, H. Wagatsuma, "Artificial neural network approach to guarantee the positioning accuracy of moving robots by using the integration of IMU/UWB with motion capture system data fusion," *Sensors*, vol. 22, no. 15, p. 5737, Jul. 2022.

[11] S. Salimpour, P.T. Morón, X. Yu, T. Westerlund, J. Peña-Queralta, "Exploiting redundancy for UWB anomaly detection in infrastructure-free multi-robot relative localization," *Front. Robot. AI*, vol. 10, p. 1190296, Dec. 2023.

[12] M. Nattke, R. Rotta, R. Natarov, O. Archila, P. Mykytyn, "Precise sensors for localization in the drone swarm," in *Proc. iCCCâiCampus Cottbus Conf.*, 2024.

[13] W. Zhao, A. Goudar, M. Tang, X. Qiao, A.P. Schoellig, "Uncertainty-aware Gaussian mixture model for UWB time difference of arrival localization in cluttered environments," in *Proc. IEEE/RSJ Int. Conf. Intell. Robots Syst. (IROS)*, Oct. 2023, pp. 5266â5273.

[14] F.B. Sorbelli, C.M. Pinotti, S. Silvestri, S.K. Das, "Measurement errors in range-based localization algorithms for UAVs: Analysis and experimentation," *IEEE Trans. Mobile Comput.*, vol. 21, no. 4, pp. 1291â1304, Sep. 2020.

[15] OptiTrack, "PrimeX 13 Motion Capture Camera," OptiTrack Website, `https://optitrack.com/cameras/primex-13/`, accessed July 14, 2025.

[16] Bitcraze, "Crazyflie 2.1 Open Source Drone," Bitcraze Website, `https://www.bitcraze.io/products/old-products/crazyflie-2-1/`, (July 2025).

[17] OptiTrack, "NatNet SDK," OptiTrack Website, `https://optitrack.com/software/natnet-sdk/`, (July 2025).

[18] Bitcraze, "Crazyradio 2.0," Bitcraze Website, `https://www.bitcraze.io/products/crazyradio-2-0/`, (July 2025).

[19] C. Chen and S. S. Kia, "OptiTrack-Aided Supervised Learning for Neural Network-Based Ultra-Wideband Ranging Bias Correction," *IEEE Sensors Journal*, vol. 24, no. 6, pp. 8484–8492, 2024.